복합적층판의 비선형 불규칙 진동 해석에 관한 고전 이론, 1차 및 3차 전단 이론의 비교 연구

Nonlinear Random Vibration of Laminated Composite Plates by Comparison of Classical Theory, 1st and 3rd Order Shear Theories

강 주 원*
Kang, Joowon

요 지

새로운 공학재료의 하나인 복합재료는 뛰어난 역학적 성질로 인해 공학 전 분야에 걸쳐 사용이 점진적으로 증가하고 있다. 이 복합재료에 대한 개발뿐만 아니라 정적 혹은 동적 하중을 받는 복합 구조물의 연구는 많이 수행되어 왔고 대부분 가해지는 하중은 확정적인 것으로 가정되었다. 그러나 실제 많은 상황에 있어 구조물에 가해지는 하중의 성질은 불규칙적이다. 본 연구에서는 불규칙 진동을 받는 복합적층판의 비선형 해석을 유한요소법에 의거하여 해석하였으며 고전 판 이론과 전단변형을 고려한 1차, 3차 이론을 비교 분석하였다. 많은 복합재료들은 전단 변형에 있어 재료적인 비선형을 나타내므로 이를 본 연구에 포함하였다.

핵심용어 : 불규칙 진동, 복합적층판, 재료적 비선형

Abstract

Composites are finding increasing use in a wide variety of engineering applications due to their outstanding mechanical properties. A number of studies have focused on the development of new materials as well as the response of composite structures to static and dynamic loads by assuming the external driving forces to be deterministic. However, there are many situations in practice where the exciting forces vary randomly. In this work, the nonlinear response of laminated composite plates excited by stochastic loading is studied by the finite element method. Classical, first-order and third-order shear theories for plates are used in the finite element formulation. Since most composites exhibit significant nonlinearity in the shear stress-strain law, this is included in the present analysis.

Keywords *: random vibration, laminated composite plates, material nonlinearity*

1. Introduction

Composites have been developed and used for a great variety of engineering applications in aeronautical, mechanical and other industries over the past 20 years. Composites have outstanding mechanical properties, such as high strength to weight ratio, excellent corro-

* Member, Sungkyunkwan Institute of Science& Technology

• 이 논문에 대한 토론을 2000년 6월 30일까지 본 학회에 보내주시면 2000년 9월호에 그 결과를 게재하겠습니다.

sion resistance, very good fatigue characteristics, etc, and are being increasingly used in civil engineering application. The behavior of composite structures is significantly different from those made of conventional materials because of their anisotropic properties, which are dependent on fiber orientations. Another noticeable feature is nonlinear behavior when shear loading is involved.

In this paper, the stochastic dynamic response of laminated composite plates is studied. Classical plate theory, which neglects transverse shear deformation, has been widely used to model laminated composite plates, but is adequate only for very thin plates. Many plate theories have been proposed to include the effect of shear deformation for the thick plates, of which, the laminated version of the first-order shear deformation theory is the simplest. This theory assumes a linear distribution of the in-plane normal and shear stresses over the thickness which results in nonzero transverse shear stresses, but does not produce the nonlinear transverse shear stress distribution through the plate's thickness. Third-order shear deformation theories can overcome the limitations of the first-order theory by introducing additional degrees-of-freedom (DOF). The third order theory can account for not only transverse shear effects but also produce a parabolic variation of the transverse shear stress through the thickness of the plate.

In this work, random vibration analysis of laminated composite plates exhibiting material nonlinearity by finite element method is performed, and results obtained using classical theory, first-order, and third-order shear theories are compared.

2. Nonlinear Constitutive Equations

Based on experimental results[1], it is well known that a unidirectional lamina displays essentially linear behavior when the direction of loading is parallel to or perpendicular to the fiber direction. However, when loaded in shear, the behavior is significantly nonlinear. Several nonlinear constitutive models have been proposed, of which the Hahn and Tsai model[1] is simple and easily implemented into a finite element formulation. In this work the proposed model can be expressed as:

$$\{\varepsilon'\} = [S]\{\sigma'\} + [0 \;\; 0 \;\; S_{44}^{*}\tau_4^3 \;\; S_{55}^{*}\tau_5^3 \;\; S_{66}^{*}\tau_6^3]^T \quad (1)$$

in which $\{\varepsilon'\} = [\varepsilon_1 \; \varepsilon_2 \; \gamma_4 \; \gamma_5 \; \gamma_6]$ and $\{\sigma'\} = [\sigma_1 \; \sigma_2 \; \tau_4 \; \tau_5 \; \tau_6]$ are the strain and stress vectors in material coordinates, [S] is the compliance matrix, and the last term on the right-hand side of eq. (1) represents shear nonlinearities. By inverting and rearranging eq. (1), the shear stress-strain law becomes

$$\{\sigma'\} = [Q]\{\varepsilon'\} + [diag\,(0,\ 0,\ f_4(\gamma_4),\ f_5(\gamma_5),\ f_6(\gamma_6))] \cdot \{\varepsilon'\} \quad (2)$$

where $[diag\,(0,\ 0,\ f_4(\gamma_4),\ f_5(\gamma_5),\ f_6(\gamma_6))]$ is the diagonal matrix, and $[Q] = [S]^{-1}$. For eqs. (1) and (2) to be exact inverse relations, the functions $f_q(\gamma_q)$, $q=4,5,6$, are the solutions of cubic equations, and contain terms involving fractional powers of γ_q. In order to simplify the problem, it is assumed that the functions $f_q(\gamma_q)$ may be approximated using the least square method by

$$f_q(\gamma_q) = a_{q1}\gamma_q^2 + a_{q2}\gamma_q^4 + \ldots + a_{qn}\gamma_q^{2n} = \sum_{i=1}^{n} a_{qi}\gamma_q^{2i}, \quad q=4,5,6 \quad (3)$$

By suitable choice of the parameters a_{qi}, the stress-strain law can be made to approximate eq. (1) for a reasonable range of shear strains. Fig. 1 shows the in-plane shear stress-strain law given by eq. (1) for Boron/Epoxy Narmco 5505, and an approximate fit using eq. (3) with n=2. The material parameters used were: $S_{66} = 1.81 \times 10^{-10} m^2/N$, $S^*_{66} = 4.67 \times 10^{-26}\ m^6/N^3$, $a_{61} = -1.558 \times 10^{13} Pa$, and $a_{62} = 2.4171 \times 10^{16} Pa$.

The stress-strain law in terms of the global coordinate system may be written as

$$\{\sigma\} = [\overline{Q}]\{\varepsilon\} + [T]^{-1} \cdot [diag\,(0,\ 0,\ f_4(\gamma_4),\ f_5(\gamma_5),\ f_6(\gamma_6))] \cdot [T]^{-T}\{\varepsilon\} \quad (4)$$

where $\{\sigma\} = [\sigma_x, \sigma_y, \tau_{yz}, \tau_{xz}, \tau_{xy}]^T$, $\{\varepsilon\} = [\varepsilon_x, \varepsilon_y, \gamma_{yz}, \gamma_{xz}, \gamma_{xy}]^T$, $[\overline{Q}] = [T]^{-1}[Q] \cdot [T]^T$, and $[T]$ is a rotational transformation matrix.

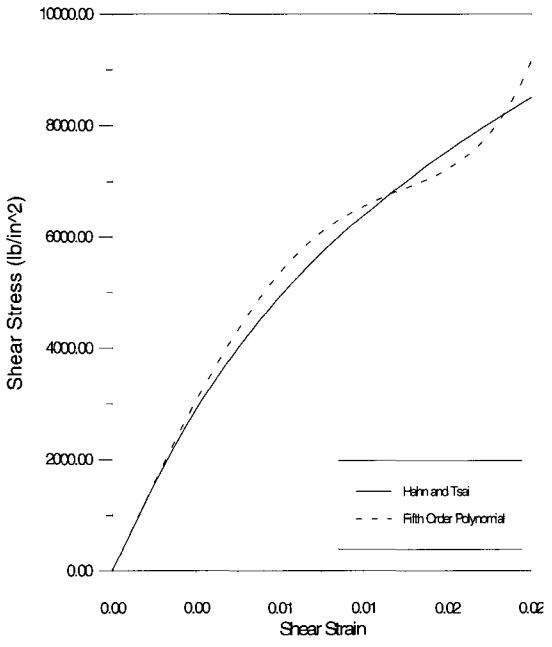

Fig. 1 Fit of approximate shear stress-strain law

3. Plate Theories

3.1 Classical Laminated Plate Theory(CLPT)

The CLPT is based on the extension of classical plate theory to laminated plates. Classical plate theory is based on Kirchhoff's hypothesis. Therefore the effect of shear deformation is neglected. Their displacements u, v, and w can be expressed as

$$\begin{aligned} u(x,y,z) &= u_0(x,y) - z\frac{\partial w}{\partial x} \\ v(x,y,z) &= v_0(x,y) - z\frac{\partial w}{\partial y} \\ w(x,y,z) &= w_0(x,y) \end{aligned} \quad (5)$$

in which u and v are in-plane displacements in the x and y directions respectively; w is the out-of-plane displacement in the z direction; u_0, v_0, and w_0 are displacements on the midplane at $z=0$; and $-\frac{\partial w}{\partial x}$ and $-\frac{\partial w}{\partial y}$ are rotational angles about the y and x directions, respectively.

3.2 First-order Shear Deformation Theory (FSDT)

A more refined plate theory that produces better results for thick plates is the FSDT. The FSDT yields a constant value of transverse shear strain through the thickness of the plate, which is an approximation. The FSDT is based on the displacement field:

$$\begin{aligned} u(x,y,z) &= u_0(x,y) + z\phi_x(x,y) \\ v(x,y,z) &= v_0(x,y) + z\phi_y(x,y) \\ w(x,y,z) &= w_0(x,y) \end{aligned} \quad (6)$$

where the additional degrees-of-freedom (DOFs) ϕ_x and ϕ_y are the rotations of the transverse normals about the y and x axes, respectively.

3.3 Third-order Shear Deformation Theory (TSDT)

While the FSDT produces acceptable results for thick plates made of traditional materials, it is not sufficiently accurate for thick composite laminated plates. The TSDT has been developed to improve accuracy[2]. In this study, a four-noded isoparametric element with seven DOFs at each node is used together with the assumed displacement field whose field indicates a cubic variation of the in-plane displacements and a parabolic distribution of the transverse shear strains through the thickness of the plate. It satisfies the stress free condition at the top and bottom surface of the plate. The assumed displacement field is

$$\begin{aligned} u(x,y,z) &= u_0(x,y) \\ &\quad + z\left[\psi_x - \frac{4}{3}\left(\frac{z}{h}\right)^2\left(\psi_x + \frac{\partial w}{\partial x}\right)\right] \\ v(x,y,z) &= v_0(x,y) \\ &\quad + z\left[\psi_y - \frac{4}{3}\left(\frac{z}{h}\right)^2\left(\psi_y + \frac{\partial w}{\partial y}\right)\right] \\ w(x,y,z) &= w_0(x,y) \end{aligned} \tag{7}$$

4. Finite Element Formulation

A four-noded rectangular plate element is used with 5 DOFs for the CLPT and 7 DOFs for FSDT and TSDT. In-plane displacements u and v are interpolated using bilinear isoparametric functions and the out-of-plane displacement w is interpolated using the nonconforming cubic functions[3]. For FSDT and TSDT, the shear rotations ψ_x and ψ_y are interpolated using bilinear isoparametric functions.

4.1 Elemental Stiffness Equation

Using a strain energy approach, the elemental stiffness equations can be obtained as

$$\{P_e\} = [K_e]\{u_e\} + \{\phi_e\} \tag{8}$$

where $[K_e]$ = linear stiffness matrix, and

$$\{\phi_e\} = \sum_{k=1}^{N}\int_{-1}^{1}\int_{-1}^{1}\int_{z_{k-1}}^{z_k}\Big([B]^T [T]^{-1}[f] \cdot [T]^{-T}[B] \cdot \{u_e\}|J|\Big)\, d\xi\, d\eta\, dz \tag{9}$$

is a nonlinear load vector arising from material nonlinearity. In eq. (9), [B] is the strain-displacement matrix in the finite element formulation, z_k is the distance from the reference plane to the bottom of the kth lamina, $|J|$ is the determinant of the Jacobian matrix for transformation from the global to the natural coordinate system and $[f] = [diag(0, 0, f_4(\gamma_4), f_5(\gamma_5), f_6(\gamma_6))$. Substituting eq. (3), eq. (9) can be written as

$$\{\phi_e\} = \sum_{k=1}^{N}\int_{-1}^{1}\int_{-1}^{1}\int_{z_{k-1}}^{z_k} [\{\phi_{4e}\}+\{\phi_{5e}\}+\{\phi_{6e}\}] \cdot \{u_e\}|J|\, d\xi\, d\eta\, dz \tag{10}$$

where $\{\phi_{qe}\} = \sum_{i=1}^{n} a_{qi}\gamma_q^{2i}[B]^T[T_q^*][B]$ and $[T_q^*] = [T]^{-1}[diag(0, 0, \delta_{q4}, \delta_{q5}, \delta_{q6}))] \cdot [T]^{-T}$ for q = 4, 5, 6 and δ_{qj} is the Kronecker delta.

4.2 Dynamic Equation of Motion

For dynamic problems, the elemental mass and damping matrices are required. Like the stiffness matrix, the consistent mass matrix can also be obtained by assembling the element mass matrices defined by

$$\begin{aligned} [M_e] &= \int_V \rho [N]^T [N]\, dV \\ &= \sum_{k=1}^{N} \rho_k \int_{-1}^{1}\int_{-1}^{1}\int_{z_{k-1}}^{z_k} [N]^T [N] \cdot |J|\, d\xi\, d\eta\, dz \end{aligned} \tag{11}$$

where ρ_k is the mass density of the kth lamina and $[N]$ contains interpolation functions. The damping matrix is usually specified indirectly through modal damping ratios. The dynamic equations of motion of a laminated plate discretized into finite elements is established as

$$[M]\{\ddot{u}\}+[C]\{\dot{u}\}+[K]\{u\}+\{\phi\}=\{P\} \quad (12)$$

where $[M]$ and $[K]$ are consistent mass and stiffness matrices obtained by assembling the element matrices, $[C]$ is the damping matrix, $\{\phi\}$ is a vector of nonlinear terms obtained by assembling the element vectors $\{\phi_e\}$, and $\{P\}$ is the external force vector.

5. Equivalent Linearization

Since exact solutions of nonlinear random vibration problems are often impossible to obtain, several approximate techniques have been developed. A method that can be used with complex finite element structural models is the method of equivalent linearization[4]. In this method, the nonlinear equation of motion given by eq. (12) is replaced by an equivalent linear one

$$[M\{\ddot{u}\}]+[C]\{\dot{u}\}+([K]+[K^*])\{u\}=\{P\} \quad (13)$$

where $[K^*]$ is the equivalent stiffness matrix related to $\{\phi\}$. $[K^*]$ is determined by minimizing the magnitude of the difference vector $\{e\}=\{\phi\}-[K^*]\{u\}$ between the actual system of equation and the equivalent linear system. Assuming that $\{P\}$ and $\{u\}$ are zero-mean Gaussian random vectors, it can be shown that the equivalent stiffness matrix, $[K^*]$ is related to the nonlinear vector $\{\phi\}$ through

$$[K^*]=E\left[\frac{\partial\{\phi\}}{\partial\{u\}}\right] \quad (14)$$

The matrix $[K^*]$ may be assembled through equivalent element stiffness matrices given by

$$\begin{aligned}[K_e^*] &= E\left[\frac{\partial\{\phi_e\}}{\partial\{u_e\}}\right] \\ &= \sum_{q=4}^{6}\sum_{k=1}^{N}\sum_{i=1}^{n}\int_{-1}^{1}\int_{-1}^{1}\int_{z_{k-1}}^{z_k}[B]^T[T_q^*] \\ &\quad\cdot[B]E\left[\frac{\partial}{\partial\{u_e\}}\gamma_q^{2i}\{u_e\}\right]|J|\,d\xi d\eta dz\end{aligned} \quad (15)$$

Substituting $\gamma_q=[T_{q-1}][B][u_e]$ from the strain-displacement relations, where $[T_{q-1}]$ is the (q-1)th row of $[T]^{-T}$, the expectation in eq. (15) becomes

$$\left[\frac{\partial}{\partial\{u_e\}}\gamma_q^{2i}\{u_e\}\right]=\alpha_q[I]+2i\{\beta_q\}[T_{q-1}][B] \quad (16)$$

where

$$\begin{aligned}\alpha_q = &\sum_{j_1=1}^{5}\sum_{k_1=1}^{28}\sum_{j_2=1}^{5}\sum_{k_2=1}^{28}\cdots\sum_{j_{2i}=1}^{5}\sum_{k_{2i}=1}^{28} \\ &(E[u_{e,k_1}u_{e,k_2}\cdots u_{e,k_{2i}}] \\ &\cdot\left\{\prod_{m=1}^{2i}T_{(q-1)j_m}\right\}\left\{\prod_{m=1}^{2i}B_{j_m k_m}\right\})\end{aligned} \quad (17)$$

and the pth element of $[\beta_q]$ is

$$\begin{aligned}\beta_{q,p} = &\sum_{j_1=1}^{5}\sum_{k_1=1}^{28}\sum_{j_2=1}^{5}\sum_{k_2=1}^{28}\cdots\sum_{j_{2i-1}=1}^{5}\sum_{k_{2i-1}=1}^{28} \\ &(E[u_{e,p}u_{e,k_1}u_{e,k_2}\cdots u_{e,k_{2i-1}}] \\ &\cdot\left\{\prod_{m=1}^{2i-1}T_{(q-1)j_m}\right\}\left\{\prod_{m=1}^{2i-1}B_{j_m k_m}\right\})\end{aligned} \quad (18)$$

6. Random Vibration Analysis

Random vibration analysis to solve eq. (13)

is performed using an iterative approach with each iteration consisting of a linear analysis. The matrix in any given iteration is computed using the nodal displacement covariances from the previous iteration and the iterations are terminated when the covariances converge. The main steps in a frequency domain approach are as follows:

Step 1. Using the mass matrix $[M]$ and the stiffness matrix $[K]+[K^*]$, where $[K^*]=0$ in the very first iteration, determine undamped natural frequencies, ω_j, and mode shape mätrices, $\{\psi_j\}$, for a chosen number of modes.

Step 2. Perform a linear random vibration analysis to determine the covariances of the nodal displacement. If the excitation P is taken to be a stationary random process, the covariances of the stationary response may be computed through

$$E[u_r u_s] = \sum_{j=1}^{n}\sum_{k=1}^{n}\frac{\psi_{rj}\psi_{sk}}{M_j M_k} \cdot \sum_{l=1}^{n}\sum_{m=1}^{n}\int_{-\infty}^{\infty} H_j(-\omega)H_k(\omega) \cdot S_{lm}(\omega)\,d\omega \tag{19}$$

where ψ_{rj} are rjth elements of the mode shape matrix, $M_j = \{\psi_j\}^T[M]\{\psi_j\}$ is the jth modal mass. $H_j(\omega)$ is the modal frequency response function for mode j given by

$$H_j(\omega) = \frac{1}{\omega_j^2 - \omega^2 + 2i\,\zeta_j\omega_j\omega} \tag{20}$$

in which ω_j and ζ_j are the undamped natural frequency and damping ratio of mode j, respectively. $H_j(-\omega)$ is the complex conjugate of $H_j(\omega)$. $S_{lm}(\omega)$ is the cross spectral density function of the nodal force excitations P_l and P_m at the lth and mth DOF.

Step 3. Compute the equivalent element stiffness matrices and assemble the global equivalent stiffness matrix.

The three steps outlined above are repeated until convergence is obtained in the covariances of nodal displacements. It is convenient to check for convergence by using the nodal displacement variances and the mth iteration is assumed to have converged if

$$\frac{\sqrt{\sum_i (\sigma_{u_i,m} - \sigma_{u_i,m-1})^2}}{\sqrt{\sum_i (\sigma_{u_i,m})^2}} \le tolerance \tag{21}$$

where $u_i = \sqrt{E[u_i^2]}$.

7. Numerical Examples

A cantilevered laminated plate having a three-ply configuration and rectangular geometry is considered. The plate is 1m long, 0.5m wide, and 0.1m thick, yielding a length to thickness ratio of L/h = 10. The thickness was chosen to be sufficiently large so that shear deformations could be significant and in reality each lamina would be composed of several sublayers. A symmetric ply arrangement with fiber orientations of α°, 0° and α° in the three plies is examined. Two values of 30° and 60° are used for comparative purposes. Each layer within the plate is modeled with nine finite elements of equal size as shown in Fig. 2.

The four nodes at the free end of the cantilever are loaded with identical loads in the z-direction, with P being a zero-mean white noise excitation. The level of the excitation spectrum was increased from 10,000 N^2s to 100,000 N^2s and the root-mean-square (RMS) responses were computed. The composite material is taken to be Boron/Epoxy Narmco 5505.

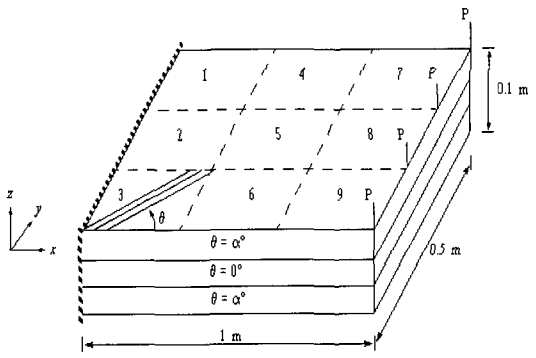

Fig 2 Three-ply symmetric laminated plate loaded in flexure

Table 1 Natural frequencies predicted by the three theories for the excitation intensity S_0 = 100,000 N^2·sec

Mode	[30° / 0° / 30°]			[60° / 0° / 60°]		
	TSDT (Hz)	FSDT (Hz)	CLPT (Hz)	TSDT (Hz)	FSDT (Hz)	CLPT (Hz)
1	84.97	84.66	88.02	59.63	59.15	60.09
2	331.66	335.56	376.79	260.47	273.64	299.20
3	490.56	493.75	493.85	381.26	358.52	377.06
4	493.95	548.36	654.29	440.02	441.84	441.92
5	934.98	939.84	1106.18	840.25	872.58	993.46

The assumed material properties were taken to be E_{11} = 205 GPa, E_{22} = 19 GPa, G_{12} = G_{13} = 6 GPa, and G_{23} = 4 GPa. The fifth order approximation shown in Fig 1 was used to approximate the nonlinear shear stress strain relations with a_{q1} = -1.558 × 10^{-13}Pa and a_{q2} = 2,417 × 10^{16}Pa. The assumed mass density was 2000kg/m^3. Results obtained using CLPT and FSDT are compared to those obtained using TSDT.

Table 1 shows the first five undamped natural frequencies of the plate from the last iteration of the analysis at the excitation level S_0 = 100,000 N^2 s for TSDT, FSDT, and CLPT. The natural frequencies obtained by the CLPT are larger than those resulting from the FSDT, which in turn are larger than those resulting from TSDT. The differences between CLPT and TSDT are as high as 32% for some frequencies. The difference in natural frequencies between the FSDT and TSDT are within 10%. Inclusion of shear deformation through progressively higher order theories therefore yields more flexible models.

The variations of the normalized RMS z-displacement at the free right corner node of the plate with the excitation load level as predicted by the different theories are shown in Fig. 3.

The normalization has been performed by dividing each response by the nonlinear response resulting from the TSDT at the same load level. The figure indicates that the displacement from the CLPT is less than that from the TSDT. At any given load level the displacements increase with the order of the theory, i.e., C L P T→F S D T→T S D T.

The variation of the normalized RMS normal stresses iof element 2 of the plate with the excitation level as predicted by the different theories are shown in Figs. 4 and 5. The behavior of the stresses is opposite to that of the displace- ments with the normal stresses resulting from CLPT and FSDT being larger than those resulting from the TSDT.

The variation of the normalized RMS shear stresses in material directions from the different theories at the center of element 2 of the plate with the excitation level are shown in Figs. 6, 7, and 8.

Fig. 6 indicates that the normalized in-plane shear stresses for 30° for the FSDT and CLPT are larger than that for the TSDT, while for 60° the reverse is true. Fig. 7 and 8 show that the transverse shear stresses predicted by the FSDT are significantly lower than those predicted

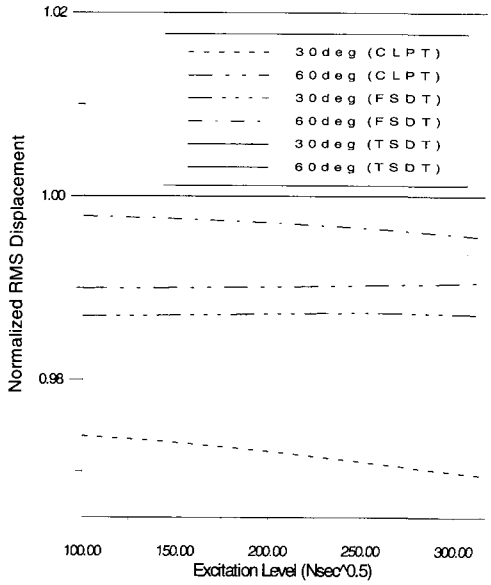

Fig. 3 Variation of normalized RMS displacement with excitation level

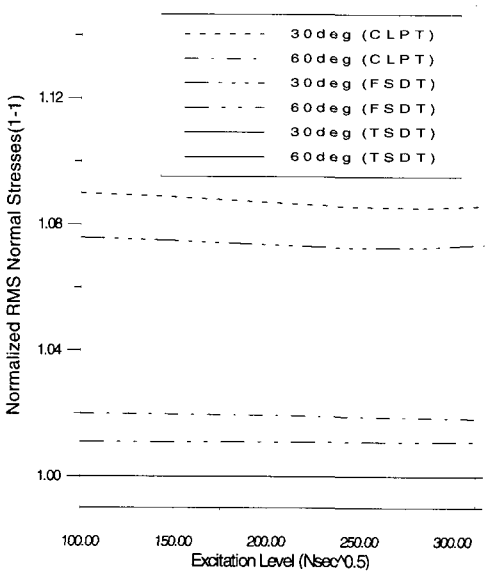

Fig. 4 Variation of normalized RMS σ_{11} with excitation level

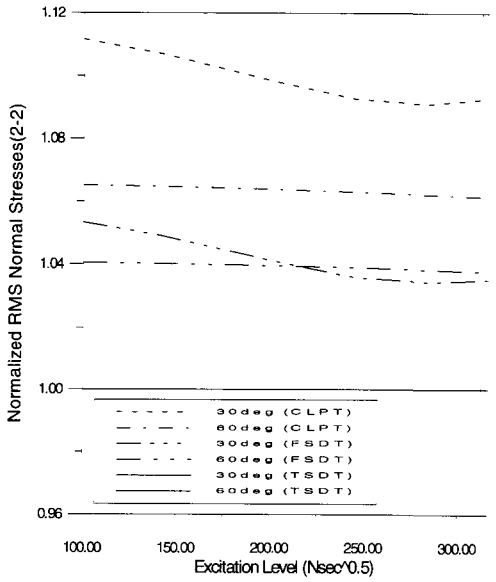

Fig. 5 Variation of normalized RMS σ_{22} with excitation level

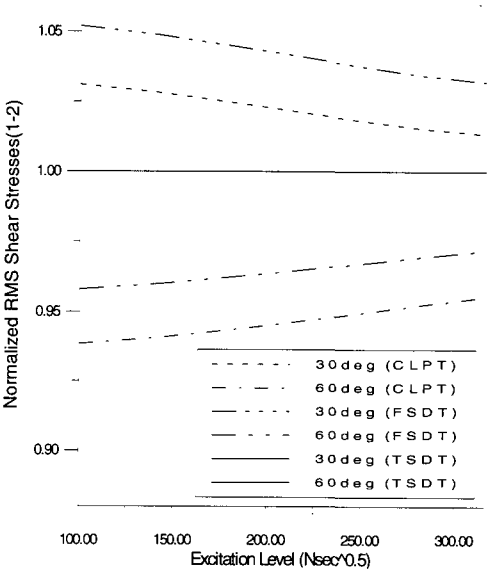

Fig. 6 Variation of normalized RMS τ_{12} with excitation level

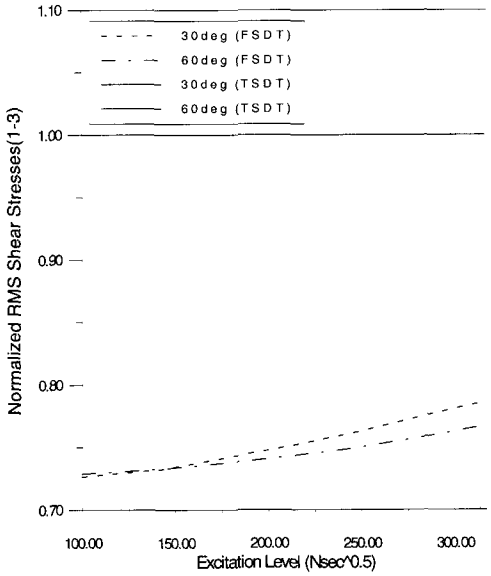

Fig .7 Variation of normalized RMS τ_{13} with excitation level

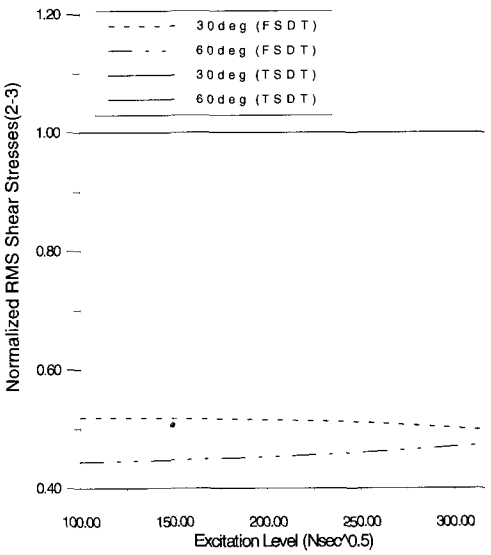

Fig. 8 Variation of normalized RMS τ_{23} with excitation level

by the TSDT. This is because the FSDT yields constant transverse shear stresses having approximately average values. Again it is apparent that the constant stresses in each layer predicted by FSDT are significantly smaller than the maximum value predicted by the TSDT.

8. Conclusions

A random vibration analysis technique for laminated composite plates modeled with finite elements and including material nonlinearity is presented. Since the shear stress-strain response of a lamina is clearly nonlinear, this feature is considered in the analysis. For expediency, an approximate nonlinear shear stress-strain law expressed in terms of a fifth-order polynomial is used to approximate the nonlinear shear stress-strain law. Since transverse shear deformation is important for even moderately thick composite plates, the TSDT which has cubic displacement fields is used. The numerical example presented indicates that the effect of nonlinearity on the responses becomes more pronounced as the excitation level is increased. This study indicates that the nonlinear shear stress-strain law produces significant nonlinearity in some displacement and stress responses depending on the fiber orientations.

The RMS responses obtained from the CLPT and the FSDT are compared with those obtained from the TSDT. The structural model becomes progressively more flexible as progressively higher-order shear theories are used. Of the three theories considered, the TSDT yields the largest displacements while the CLPT yields the smallest displacements.

Transverse shear stresses predicted by the FSDT are significantly smaller than those predicted by the TSDT.

The versatility of the nonlinear random vibration method developed is that it can be applied to laminated composite plates with

complex geometries and excitations with varying degrees of elastic nonlinearity in the shear stress-strain law.

References

1. Hahn, H. T. and Tsai, S. W., "Nonlinear Elastic Behavior of Unidirectional Composite Laminae," *Journal of Composite Materials*, 7, 1973, pp.102~118
2. Reddy, J. N., "A Simple Higher-order Theory for Laminated Composite Plates," *Journal of Applied Mechanics*, 51, 1984, pp.745~752
3. Zienkiewicz, O. C. and Cheung, Y. K., "The Finite Element Method for Analysis of Elastic Isotropic and Orthotropic Slabs," *Proceedings of the Institute of Civil Engineers*, 28, 1964, pp.471~488
4. Socha, L. and Soong, T. T., "Linearization in Analysis of Nonlinear Stochastic Systems," *Applied Mechanics Review*, 44, 1991, pp.399~422
5. Harichandran, R. S., "Random Vibration under Propagating Excitation: Closed-form Solutions," *Journal of Engineering Mechanics, ASCE*, 118(3), 1992, pp.575~586
6. Kang, J. and Harichandran, R. S., "Nonlinear Random Vibration of Laminated Composite Plates using High-order Shear Theory," *Proceedings, 7th International Conference on Computing in Civil and Building Engineering*, Vol. 2, 1997, pp.1133~1138

(접수일자 : 1999. 11. 17)